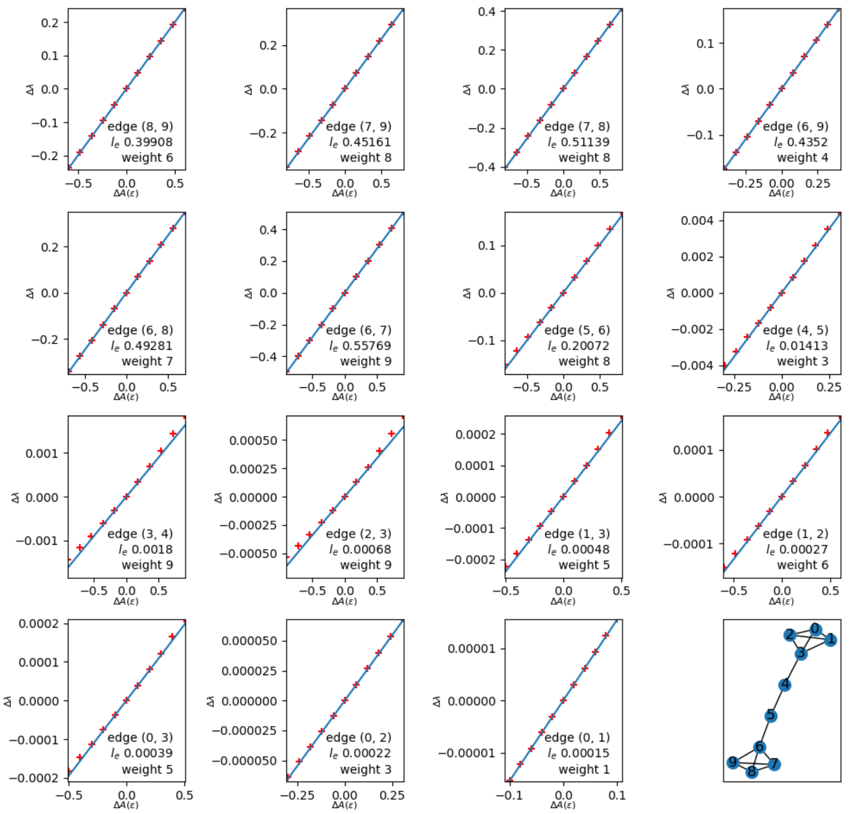

Figure 1 Scatter plot of perturbations ΔA_{ij} and the resulting $\Delta\lambda$, compared to line of constant l_e. Weighted barbell network

1 Results of perturbing two nodes in toy networks

The plots shown in figures 1 - 3 show additional results for the case of perturbing single edges for weighted barbell networks, and unweighted ring and Erdős–Rényi networks.

In figures 4 - 8 we present the results of changing two individual edges, and observing the resulting change in λ for the range of perturbations applied. We overlay this with a line of constant l_e, to assess the performance of our approximation.

2 Perturbation theory approach to deriving network eigenvalue derivatives

2.1 Undirected case

Consider a perturbation to the adjacency matrix $\mathbf{A}$:

$$\mathbf{A} \to \mathbf{A} + \epsilon\mathbf{B} \tag{1}$$

and the resulting first order changes to the leading eigenvalue λ and the associated eigenvector $|\lambda\rangle$:

$$\lambda = \lambda_0 + \epsilon\lambda \tag{2}$$

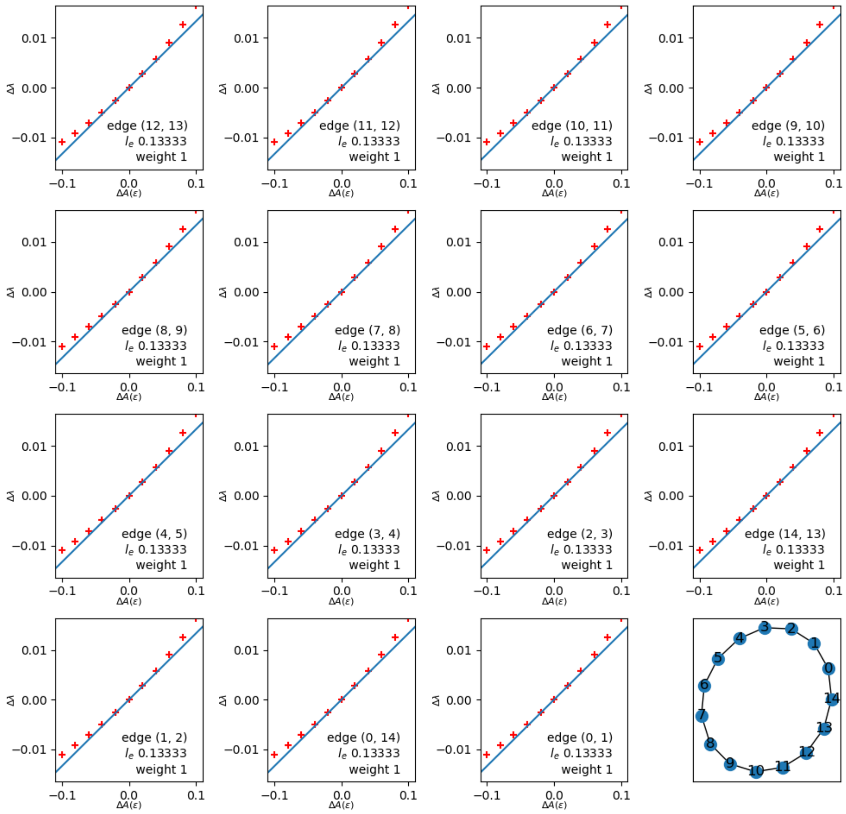

Figure 2 Scatter plot of perturbations ΔA_{ij} and the resulting $\Delta\lambda$, compared to line of constant l_e. Unweighted ring network.

$$|\lambda\rangle = |\lambda\rangle_0 + \epsilon\,|\lambda\rangle_1 \tag{3}$$

Substituting these into our eigenvalue equation

$$(\mathbf{A} + \epsilon\mathbf{B})(|\lambda\rangle_0 + \epsilon\,|\lambda\rangle_1) = (\lambda_0 + \epsilon\lambda_1 + ...)(|\lambda\rangle_0 + \epsilon\,|\lambda\rangle_1 + ...) \tag{4}$$

and considering terms up to 1st order in ϵ

$$\mathbf{A}\,|\lambda\rangle_0 + \epsilon\mathbf{B}\,|\lambda\rangle_0 + \epsilon\mathbf{A}\,|\lambda\rangle_1 = \lambda_0\,|\lambda\rangle_0 + \epsilon\lambda_1\,|\lambda\rangle_0 + \epsilon\lambda_0\,|\lambda\rangle_1 \tag{5}$$

Then we can consider each of the terms in ϵ^n separately,

$$\epsilon_0 : \mathbf{A}\,|\lambda\rangle_0 = \lambda_0\,|\lambda\rangle_0 \tag{6}$$

$$\epsilon_1 : \mathbf{B}\,|\lambda\rangle_0 + \mathbf{A}\,|\lambda\rangle_1 = \lambda_1\,|\lambda\rangle_0 + \lambda_0\,|\lambda\rangle_1 \tag{7}$$

By multiplying the equation for ϵ^1 by the left eigenvector ${}_0\langle\lambda|$, and making use of the hermitian properties of $\mathbf{A}$ such that ${}_0\langle\lambda|\mathbf{A} = \lambda_0\,{}_0\langle\lambda|$, we find

$${}_0\langle\lambda|\mathbf{B}|\lambda\rangle_0 = \lambda_1\,{}_0\langle\lambda|\lambda\rangle_0 \tag{8}$$

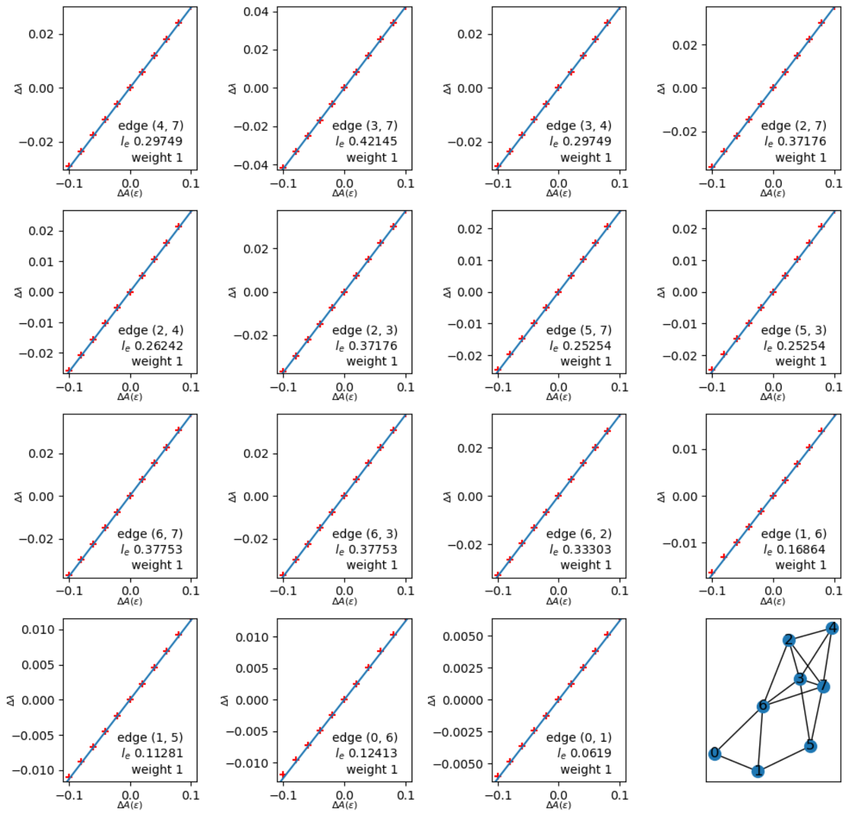

Figure 3 Scatter plot of perturbations ΔA_{ij} and the resulting $\Delta\lambda$, compared to line of constant l_e. Unweighted Erdős–Rényi network

The perturbation we are considering is changing one row, and one column, i.e. where $B_{ij} = A_{ij}$ if i or j are the row/column we are changing, zero otherwise:

$$B_{ij} = \begin{cases} A_{ij} & \text{if } i = k \text{ or } j = k \\ 0 & \text{otherwise} \end{cases}$$

Then, expanding the indices,

$$\sum_{ij} \lambda_{0,i} B_{ij} \lambda_{0,j} = \sum_{ij} \lambda_{0,i} A_{ij} \lambda_{0,j} \delta_{ik} + \sum_{ij} \lambda_{0,i} A_{ij} \lambda_{0,j} \delta_{jk} = 2 \sum_{j} \lambda_{0,k} A_{kj} \lambda_{0,j} \quad (9)$$

Where we have re-labelled the indices for the second term and have evaluated the δ's. Leading us to the result:

$$l_e = \frac{\partial \lambda}{\partial A_{ij}} = 2\lambda_{0,i}\lambda_{0,j} \quad (10)$$

where $\lambda_{0,i}$ is the ith component of the eigenvector corresponding to the leading eigenvalue of $\mathbf{A}$

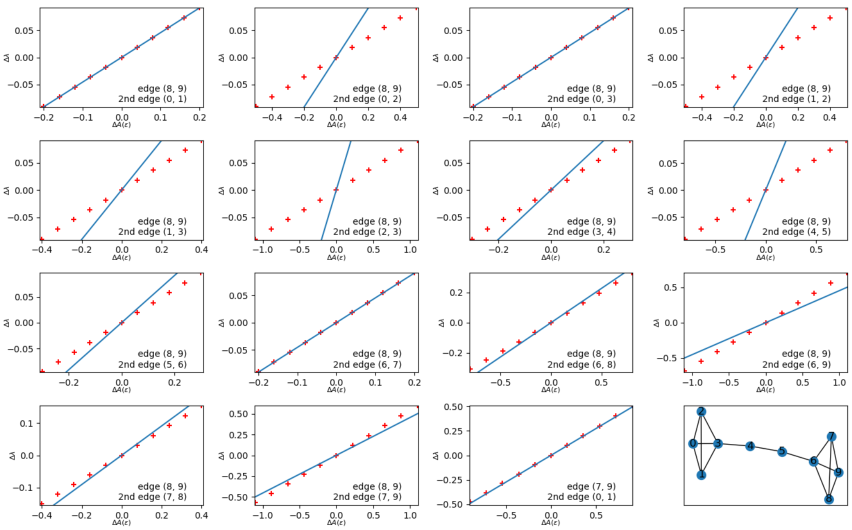

Figure 4 Scatter plot of perturbations ΔA_{ij} and the resulting $\Delta\lambda$, compared to line of constant l_e, for the case of two edges changing. The plots consider one of the two perturbed edges. Barbell network, with equal initial weights

2.2 Directed case

For the directed case, we still have that

$$\epsilon_1 : \mathbf{B} \left|\lambda\right\rangle_1 + \mathbf{A} \left|\lambda\right\rangle_0 = \lambda_1 \left|\lambda\right\rangle_0 + \lambda_0 \left|\lambda\right\rangle_1 \tag{11}$$

but we can't use the hermitian properties of the matrix $\mathbf{A}$ as for directed networks $\mathbf{A}$ is generally not symmetric. We can however consider the matrix $\mathbf{M} = \mathbf{A}\mathbf{A}^{\mathbf{T}}$ and perturbation $\mathbf{M} \to \mathbf{M} + \epsilon\mathbf{C}$, and use the symmetric result from this. This is useful since the singular values of matrix $\mathbf{A}$ are defined as the square root of the eigenvalues of $\mathbf{A}\mathbf{A}^{\mathbf{T}}$, such that:

$$\partial\lambda^M = 2s^A \partial s^A \tag{12}$$

where λ^M is the leading eigenvalue of $\mathbf{M}$ and s^A is the leading singular value of $\mathbf{A}$. We can then make use of our result above for the symmetric matrix,

$${}_0\langle\lambda^M|\mathbf{C}|\lambda^M\rangle_0 = \lambda_1^M \tag{13}$$

Where ${}_0\langle\lambda^M|$ and $|\lambda^M\rangle_0$ are the left and right eigenvectors of $\mathbf{M}$. For the directed case, our perturbation is changing just a row (or column) independently, i.e.

$$C_{ij} = \Big\{ M_{ij} \text{ if } i = k \quad 0 \text{ otherwise} \tag{14}$$

Then, expanding the indices,

$$\sum_{ij} \lambda_{0,i}^M C_{ij} \lambda_{0,j}^M = \sum_{ij} \lambda_{0,i}^M M_{ij} \lambda_{0,j}^M \delta_{ik} = \sum_j \lambda_{0,k}^M M_{kj} \lambda_{0,j}^M \tag{15}$$

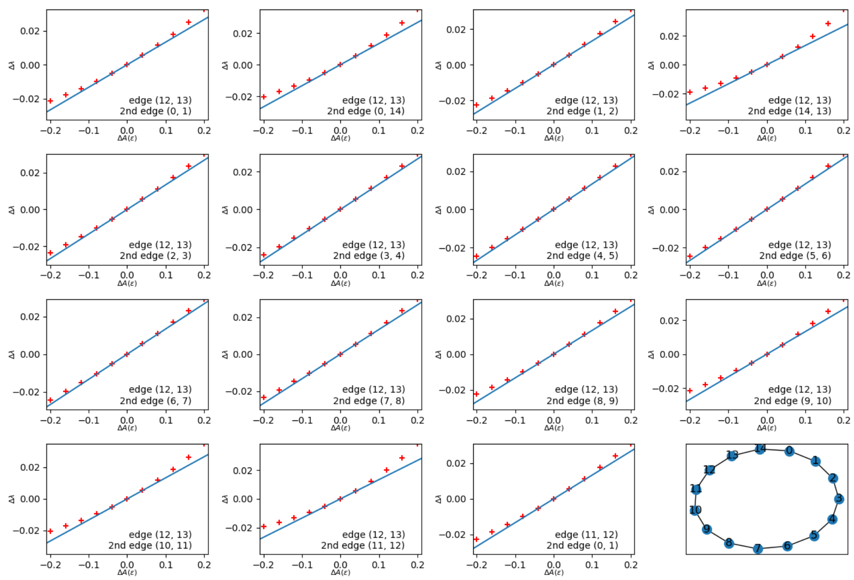

Figure 5 Scatter plot of perturbations ΔA_{ij} and the resulting $\Delta\lambda$, compared to line of constant l_e, for the case of two edges changing. The plots consider one of the two perturbed edges. Ring network with randomly assigned weights.

Leading us to the result

$$\frac{\partial s^A}{\partial M_{ij}} = \frac{\lambda^M_{0,i}\lambda^M_{0,j}}{2s^A} \tag{16}$$

where $\lambda^M_{0,i}$ is the ith component of the eigenvector corresponding to the leading eigenvalue of $\mathbf{M}$ In both the directed and undirected case above, it is worth noting that the derivations can be generalised to allow new links to be added/removed, however new nodes cannot be added or removed.

3 Kernel Density Estimation for conditional probability estimation

We make use of multivariate conditional Kernel Density Estimation (KDE) to find the probability distributions for the values of l_e. The functional form of the KDE is

$$\hat{f}_h(x) = \frac{1}{n}\sum_{i=1}^{n}\mathcal{K}_h(x-x_i) = \frac{1}{nh}\sum_{i=1}^{n}\mathcal{K}\left(\frac{(x-x_i)}{h}\right) \tag{17}$$

where

$$\mathcal{K}_h(x) = \frac{1}{h}\mathcal{K}\frac{x}{h} \tag{18}$$

is the kernel function, a non-negative function. The parameter h is the bandwith, a smoothing parameter. We have used a Gaussian kernel:

$$\mathcal{K} = \frac{1}{\sigma\sqrt{2\pi}}\exp -\frac{1}{2}\left(\frac{x-\mu}{\sigma}\right) \tag{19}$$

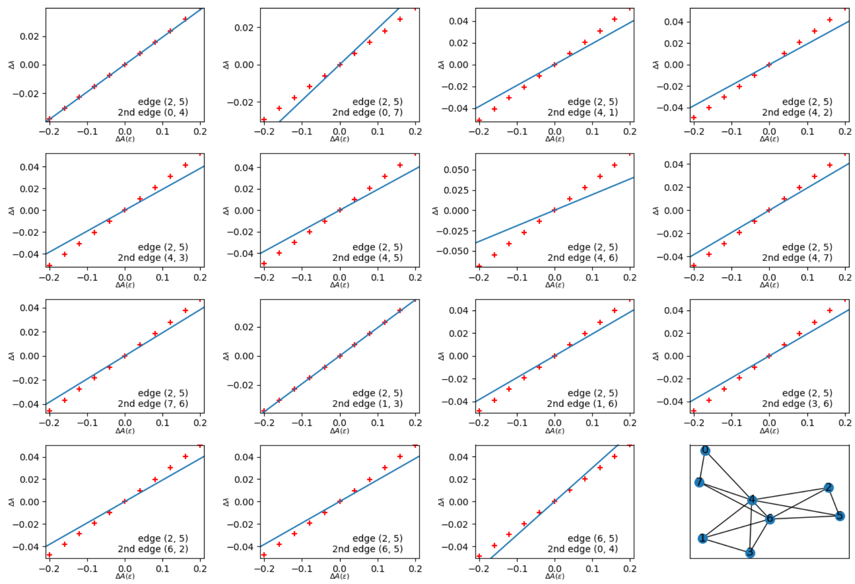

Figure 6 Scatter plot of perturbations ΔA_{ij} and the resulting $\Delta\lambda$, compared to line of constant l_e, for the case of two edges changing. The plots consider one of the two perturbed edges. Erdős–Rényi network with randomly assigned weights

4 Dataset descriptions

The first dataset considered tracks bilateral trade flows between states from 1870-2014, describing import and export data in current U.S. dollars for pairs of sovereign states [1]. This dataset is interesting not just due to its relevance to our focus on financial markets, but also due to an observed growth across time, apart from in two time periods corresponding to the First and Second World Wars.

The second dataset considered was a dataset of private messages sent on an online social network at the University of California. An edge (u, v, t) means that user u sent a private message to user v at time t. As this network is unweighted, the weights of all of the edges have been set to 1. The network was aggregated to daily snapshots, in which the edge weight is the number of times that edge is active during that day.

Finally, in order to observe the effects of different trading structures on the output of our methods, we applied our techniques to transaction reports relating to three different equity stocks traded on the UK capital markets. The data was aggregated daily, and covers a 2 year period from January 2018[1]. The Equity-3 dataset was analysed for the shorter time range of 03/06/2019 to 05/11/2019. We chose to study networks of transactions for stocks on energy companies due to the high level of trading activity in is sector. The results displayed in this paper consider the giant component networks of 3 different stocks. The first two instruments were traded without the presence of CCPs, one focusing on oil and gas exploration and production and the second focusing on renewable and alternative energy. The third instrument, another oil and gas production stock, shows a network dominated by

[1]the Equity-3 dataset was analysed for a 5 month period ending in November 2019

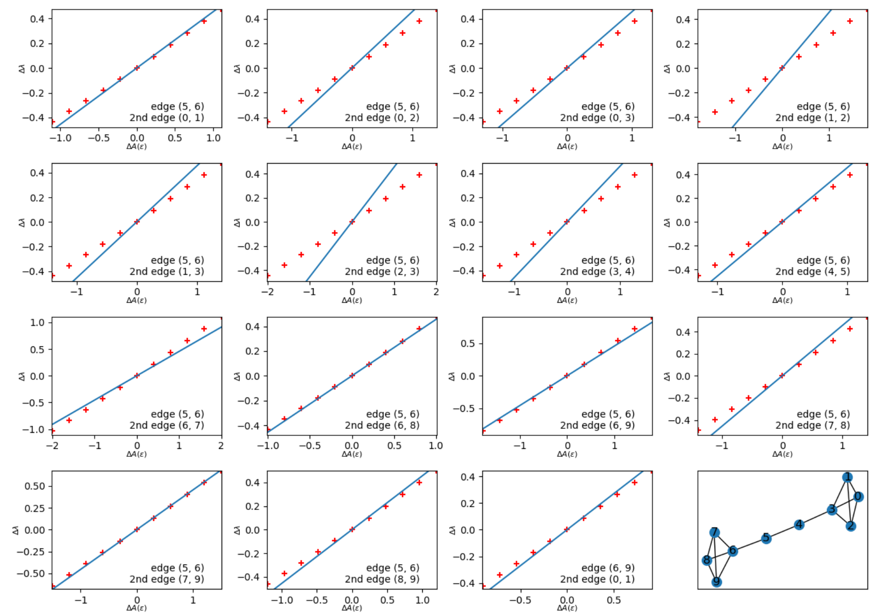

Figure 7 Scatter plot of perturbations ΔA_{ij} and the resulting $\Delta\lambda$, compared to line of constant l_e, for the case of two edges changing. The plots consider one of the two perturbed edges. Barbell network, with randomly assigned weights.

dataset	# nodes	# edges	connectivity	density	reciprocity	correlation coefficient
Equity - 1	232	6, 961	30%	12.99%	67.72	62.9%
Equity - 2	94	3,684	39.2%	42.14%	75.03%	56.84%
Equity -3	263	9.094	34.58%	13.2%	57.66%	51.23%

Table 1 Network statistics for the three Equity datasets

the presence of a CCP. Due to the sensitivity of the data, these have been referred to as Equity networks 1, 2 and 3 throughout this paper.

4.1 Summary statistics for the Equity datasets

The Equity data was made available by the FCA for use in this study, and is not publically available. To provide the reader with additional context, here we include some high level network statistics for these networks. All statistics are based on the networks following the removal of nodes which appear on less than 5 days in the sample, which we classed as 'inactive'.

We see that all three networks have similar connectivities, but Equity-3 is significantly denser than the other two and shows a higher level of reciprocity. All datasets show similar values for the correlation coefficient of the adjacency matrix.

We can see from figures 10 and 11 that large transaction values are more likely to have a high reciprocity for the first and second dataset. However the same cannot be said for the third Equity dataset, as shown in figure 12.

The evolution of high level network statistics are shown in figures 13,14, and 15. Here we see that the networks fluctuate around a relatively stable mean, with no obvious level of growth or decay across the time period.

It is further interesting to note that the third network considered shows the presence of a hierarchy in the network, due to it being an instrument that is traded

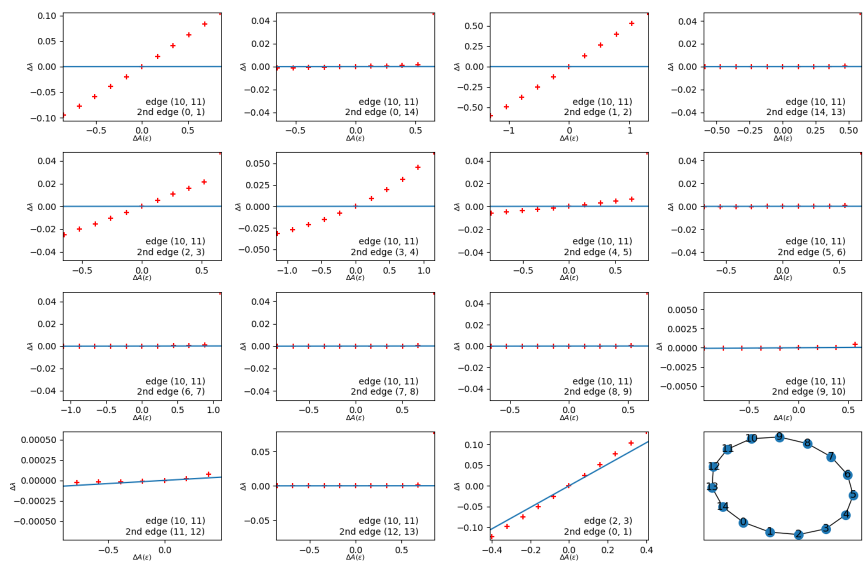

Figure 8 Scatter plot of perturbations ΔA_{ij} and the resulting $\Delta\lambda$, compared to line of constant l_e, for the case of two edges changing. The plots consider one of the two perturbed edges. Ring network with equal weights.

mainly through the use of Central Clearing Parties (CCP), producing a tiered structure as shown in figure 16. Such a structure can be identified following the identification of a dominant node in the network, i.e. a node with significantly higher degree, and examining its ego network.

5 Parameter estimations

5.1 Estimation of ρ and α

We assume in this section that our networks can be described by a model in which the probability of an edge changing is given by

$$P(\Delta) = \theta_e = \begin{cases} 0 & \alpha l_e^\rho \leq 0 \\ \alpha l_e^\rho & 0 < \alpha l_e^\rho < 1 \\ 1 & \alpha l_e^\rho \geq 1 \end{cases}$$

The maximum likelihood estimate of θ then follows the same procedure as in the case of a (potentially biased) coin toss - given a sample of changes k_i, the likelihood of observing these changes given θ is

$$L(k_1, k_2, ...k_n|\theta) = \prod_i f(k_i|\theta_i) \tag{20}$$

where $f(k_i|\theta_i)$ follows the Bernoulli distribution $\theta_e^{k_e}(1-\theta_e)^{1-k_e}$ where k_e is the observed outcome of edge e. Taking the logarithm of this, our log-likelihood is given by

$$ln(L(\mathbf{k}|\theta)) = \sum_e^N k_e ln(\theta_e) + (1-k_e) ln(1-\theta_e) \tag{21}$$

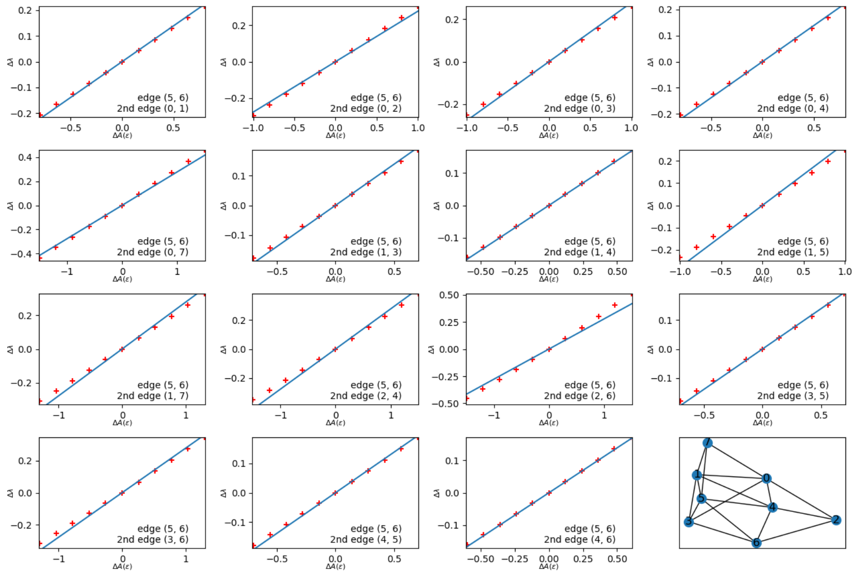

Figure 9 Scatter plot of perturbations ΔA_{ij} and the resulting $\Delta\lambda$, compared to line of constant l_e, for the case of two edges changing. The plots consider one of the two perturbed edges. Erdős–Rényi network with equal weights

Since αl_e^ρ is constrained to be a probability, to estimate the parameters which result in the maximum likelihood, we need to minimise the negative log-likelihood with respect to multiple inequality constraints:

$$0 \leq \alpha l_e^\rho \leq 1 \tag{22}$$

Where we have one inequality constraint for each l_e. To do this, we make use of the Karush-Kuhn-Tucker conditions [2] and numerical optimisation, to find the optimal saddle point which maximises L with whilst satisfying these constraints.

5.2 Estimation of β and γ

For the case of the distribution of edge changes drawn from a Gaussian distribution with μ=0 and $\sigma = \beta l_e^\gamma$, the log-likelihood is given by

$$\ln(L) = \sum_e^N \ln\left(\frac{1}{\sqrt{2\pi}\beta l_e^\gamma}\right) \exp\left(\frac{-(\Delta A_e^{rel})^2}{2\beta^2 l_e^{2\gamma}}\right) \tag{23}$$

where ΔA_e^{rel} refers to the observed relative change of edge e. Differentiating with respect to β,

$$\beta = \sqrt{\frac{1}{N}\sum_e^N \frac{(\Delta A_e^{rel})^2}{l_e^{2\gamma}}} \tag{24}$$

From which we recover the expected standard deviation for a Gaussian in the case of γ=0.

Differentiating with respect to γ,

$$\frac{\partial \ln(L)}{\partial \gamma} = \sum_{e}^{N} - \ln(l_e) + \frac{\partial}{\partial \gamma} \frac{(\Delta A_e^{rel})^2}{2\beta^2} \exp\left(-2\gamma \ln l_e\right) \tag{25}$$

which when set to 0,

$$\sum_{e}^{N} \ln(l_e) \left(1 + \frac{(\Delta A_e^{rel})^2 ln(l_e)}{\beta^2 l_e^{2\gamma}}\right) \tag{26}$$

Substituting 24 for β, and solving numerically allows us to produce an estimate for γ.

6 Comparison of data distributions to model

Figure 17 shows the bulk of the distributions for $P(\Delta A_{ij} = 0 | \ln(l_e))$ for our 5 datasets, in comparison to the equivalent generated from our model for network evolution given by equation 27:

$$A_{ij}^{t+1} = \mathcal{V}_{ij}^t A_{ij}^t \mathcal{U}_{ij}^t + (1 - \mathcal{V}_{ij}^t) A_{ij}^t \tag{27}$$

Author details

References

1. Barbieri, K., K., O.: Correlates of War Project Trade Data Set Codebook, Version 4.0. Online: http://correlatesofwar.org (2016)
2. Kuhn, H.W., Tucker, A.W.: Nonlinear programming. Proceedings of the Seconds Berkeley Symposium on Mathematical Statistics and Probability, pp. 481-492 (1950)

Reciprocity vs. price for the Equity networks

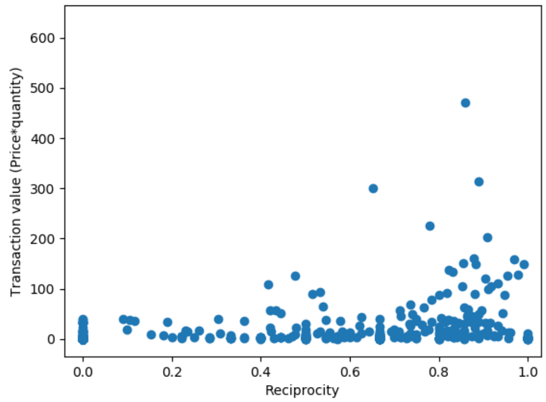

Figure 10 Equity-1

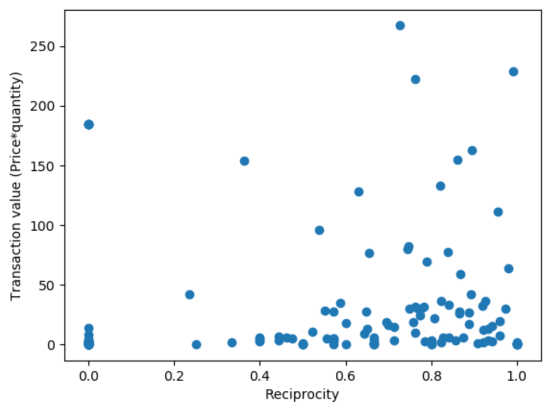

Figure 11 Equity-2

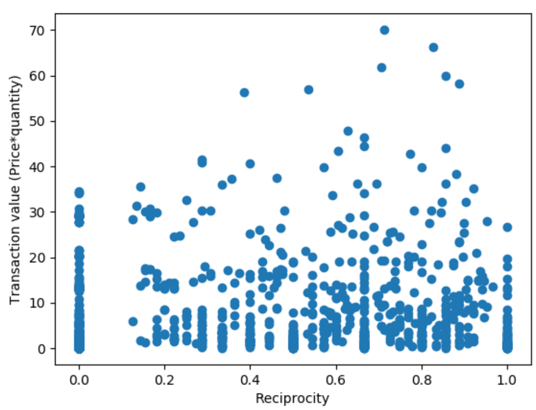

Figure 12 Equity-3

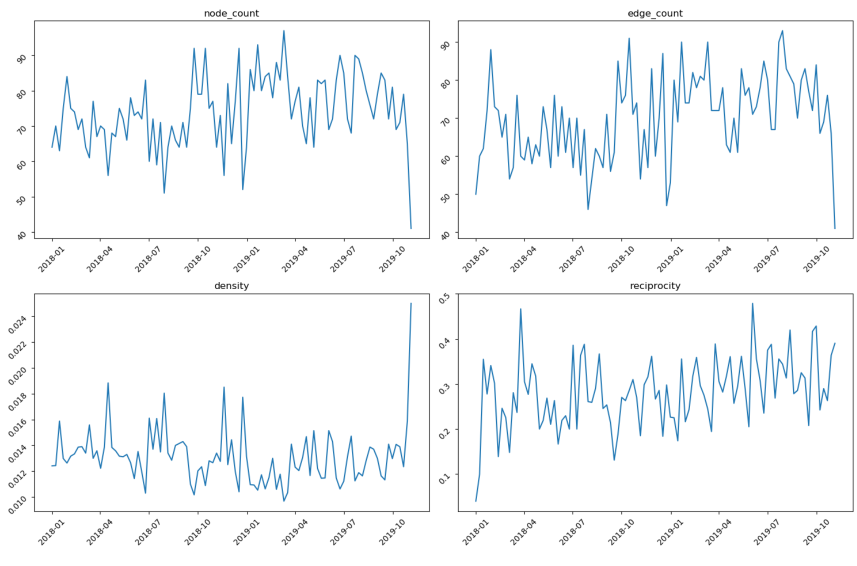

Figure 13 Daily counts of nodes and edges, density and reciprocity across the entire investigation period for Equity-3

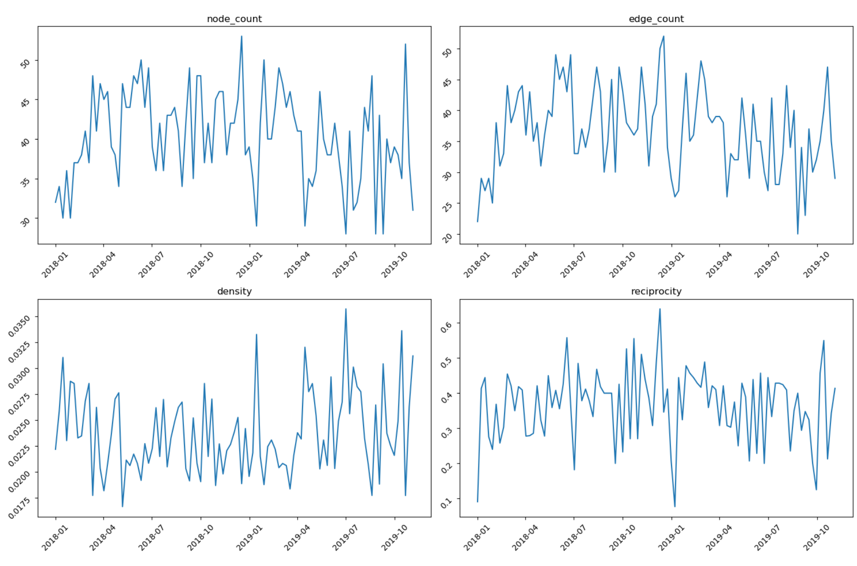

Figure 14 Daily counts of nodes and edges, density and reciprocity across the entire investigation period for Equity-2

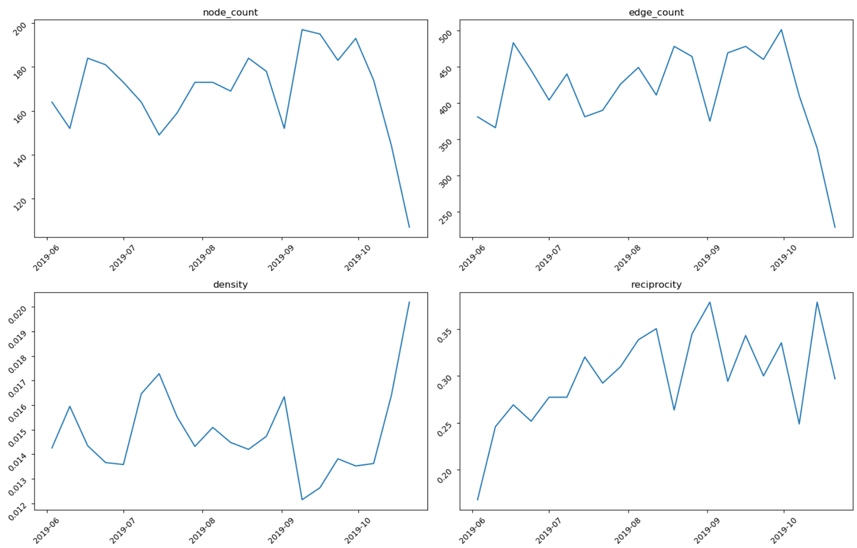

Figure 15 Daily counts of nodes and edges, density and reciprocity across the entire investigation period for Equity-3

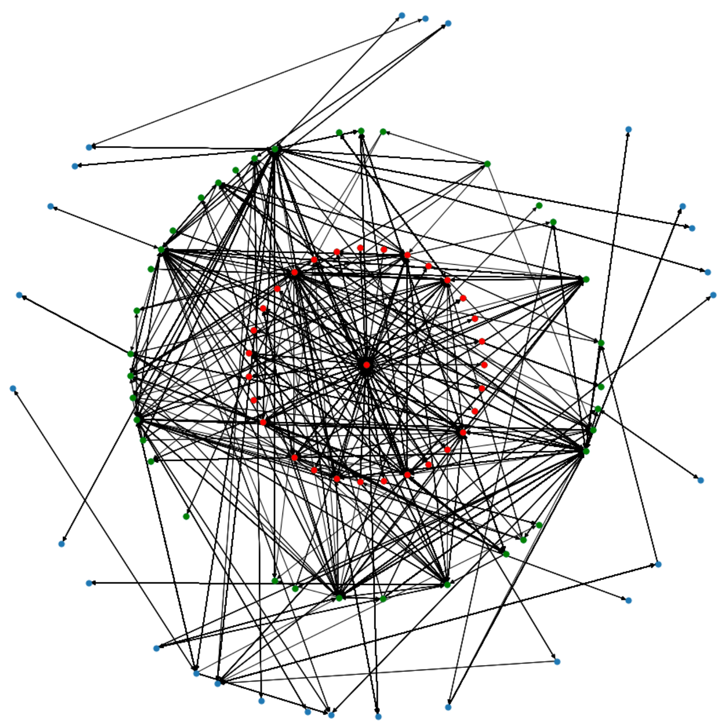

Figure 16 Example of a tiered structure in the GWCC of the trading network for an instrument frequently traded via an individual CCP.

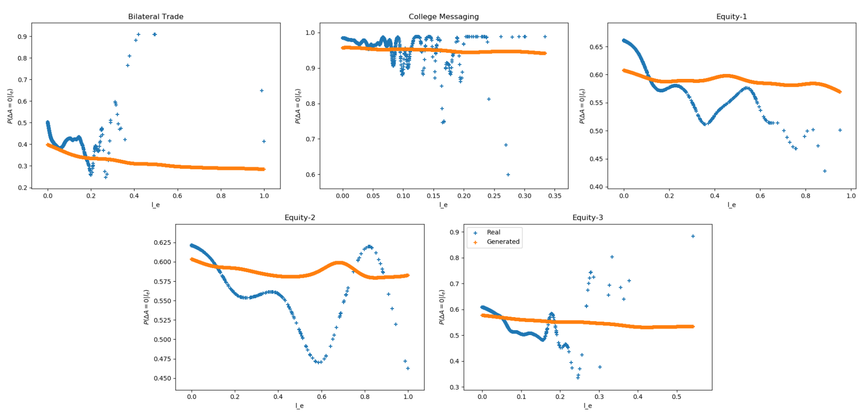

Figure 17 $P(\Delta A_{ij} = 0|\ln(l_e))$ as a function of $\ln(l_e)$ for the 5 real datasets, overlaid with the distributions for data generated according to the model in 27